



Investigations on substituted (2-aminothiazol-5-yl)(imidazo[1,2-a]pyridin-3-yl)methanones for the treatment of Alzheimer's disease

Sneha R. Sagar^{a,c,1}, Devendra Pratap Singh^{b,2}, Rajesh D. Das^a, Nirupa B. Panchal^a, Vasudevan Sudarsanam^a, Manish Nivsarkar^b, Kamala K. Vasu^{a,*}

^a Department of Medicinal Chemistry, B. V. Patel Pharmaceutical Education and Research Development (PERD) Centre, S. G. Highway, Thaltej, Ahmedabad 380054, Gujarat, India

^b Department of Pharmacology and Toxicology, B. V. Patel Pharmaceutical Education and Research Development (PERD) Centre, S. G. Highway, Thaltej, Ahmedabad 380054, Gujarat, India

^c Institute of Pharmacy, NIRMA University, S. G. Highway, Chandlodia, Gota, Ahmedabad, Gujarat 382481, India

ARTICLE INFO

Keywords:

Imidazo[1,2-a]pyridines
Thiazoles
Neuronal inflammation
Alzheimer's disease

ABSTRACT

Alzheimer's disease (AD) is a neurodegenerative disease majorly affecting old age populations. Various factors that affect the progression of the disease include, amyloid plaque formation, neurofibrillary tangles, inflammation, oxidative stress, etc. Herein we report of a new series of substituted (2-aminothiazol-5-yl)(imidazo[1,2-a]pyridin-3-yl)methanones. The designed compounds were synthesized and characterized by spectral data. *In vivo* anti-inflammatory activity was carried out for screening of anti-inflammatory potential of synthesized compounds. All the compounds were tested for acute inflammatory activity by using carrageenan induced acute inflammation model. Compounds **10b**, **10c**, and **10o** had shown promising acute anti-inflammatory activity and they were further tested for formalin induced chronic inflammation model. Compound **10c** showed both acute and chronic anti-inflammatory activity. Compound **10c** also showed promising results in AlCl₃ induced AD model. Studies on various behavioral parameters suggested improved amnesic performance of compound **10c** treated rats. Compound **10c** treated rats also exhibited excellent antioxidant and neuroprotective effect with inherent gastrointestinal safety.

1. Introduction

Alzheimer's disease (AD) is a progressive and unremitting neurodegenerative disorder of old age which affects wide areas of cerebral cortex and hippocampus. The malformations in AD are initially detected in brain tissue that involves the frontal and temporal lobes and then slowly propagates to other regions of the neocortex at different rates in different individuals.¹ The peculiar characteristics are irrevocable memory impairment, decline in cognitive ability and higher intellectual functions.¹ In 2020, World Health Organization (WHO) reported 50 million people were living with dementia globally and this figure is set to increase to 152 million by 2050.² Amidst various factors governing the pathophysiology of AD, β -amyloid (A β) deposition, τ -protein

aggregation, cholinergic neurotransmitter imbalance, oxidative stress and neuronal inflammation can be largely attributed as its hallmarks.³

In recent years, a retrospection into underlying inflammatory responses in context of AD mechanism, proposes neuronal inflammation to be a critical factor for pathogenesis of AD. Neuronal inflammation is largely manifested by the activation of microglia and astrocytes. Under normal physiological condition, microglia cells are in a state of rest.⁴ However, in neurodegenerative diseases, they are constantly activated and trigger the release of inflammatory cytokines eventually leading to chronic neuroinflammation. Studies show that these inflammatory cytokines aggravate oxidative stress in brain and stimulate the generation, aggregation and accumulation of insoluble A β plaques in extracellular spaces, as well as in walls of blood vessels.⁵ The accumulated insoluble

Abbreviations: AD, Alzheimer's disease; COXs, cyclooxygenases; RT, room temperature; NC, normal control; DC, disease control; PC, positive control; LPO, Lipid peroxidation; SOD, Superoxide dismutase.

* Corresponding author.

E-mail address: kamkva@gmail.com (K.K. Vasu).

¹ Present address: L. J. Institute of Pharmacy, S. G. Highway, Sanand Circle, Sarkhej, Ahmedabad, Gujarat 382210, India.

² Present address: Manager R&D, (FDD-NDDS), Sun Pharmaceutical Industries Limited, Tandalija, Vadodara, Gujarat, India.

<https://doi.org/10.1016/j.bmc.2021.116091>

Received 3 January 2021; Received in revised form 15 February 2021; Accepted 16 February 2021

Available online 27 February 2021

0968-0896/© 2021 Elsevier Ltd. All rights reserved.

$A\beta$ plaques induce cyclooxygenase-2 (COX-2) expression. In addition, the activation of microglia occurs before neurodegenerative symptoms appear, and this can be regarded as an early event related to pathological changes in AD. Thus, anti-inflammatory agents are considered to be potential candidates for Alzheimer's disease. Researchers showed that anti-inflammatory drugs could even control the release of inflammatory factors and oxygen free radicals caused by the deposition of $A\beta$, and reduce the amount and area of $A\beta$ deposition.⁶ However, the available literature reported controversial role of anti-inflammatory agents in the progression of AD. The reports suggested that anti-inflammatory benefits were observed only in low doses during AD pathology and some of the NSAIDs were failed to show clinical efficacy. The reason behind lower activity could be due to some factors like brain penetration of drug, pharmacological properties of drugs, dosing schedule and selection of patients.⁷

Imidazopyridine ring scaffold has been proved to be efficacious against neuroinflammation by regulating various pro-inflammatory mediators and COXs enzymes.⁸⁻¹¹ Based on this mechanism, Imidazo[1,2-*a*]pyridin-3-yl(7-methylimidazo[1,2-*a*]pyridin-3-yl)methanone (**1**) was designed and it exhibited 67% inhibition against acute inflammation and 61% inhibition of chronic inflammation in rat paw edema model.⁸ 1',3'-dihydro-2H-spiro[imidazo[1,2-*a*]pyridine-3,2'-inden]-2-one (**2**) was found to be a potent complex cognitive enhancer as it is able to influence the processes in neuroinflammation pathways.⁹ Moreover, our previous work on Imidazo[1,2-*a*]pyridines linked with thiazoles/thiophene motif through keto spacer, indicated the importance of Imidazopyridines against the progression of various inflammatory events and NF- κ B and AP-1 mediated transcriptional processes. Thiazole moiety has important structural features of having H-bond acceptor and H-bond donor.^{12,13} Methyl 3-(4-(dimethylamino)-2-(methylamino)thiazol-5-yl)-2-(methoxyimino)-3-oxopropanoate (**3**) was reported as an anti-inflammatory agent with 83% inhibition of rat paw edema in acute inflammation and 66% inhibition of rat paw edema in chronic inflammation.¹² *N,N'*-(5,5'-oxalylbis(4-methylthiazole-5,2-diyl)dibenzamide (**4**) showed 73% inhibition of edema in acute inflammation rat model.¹²

In present study, imidazo[1,2-*a*]pyridines were clubbed with thiazoles to get the beneficial effects of both the pharmacophores. Thus, we hypothesize that taking these two pharmacophores in a single molecule may increase anti-inflammatory potential of the compounds as depicted in Fig. 1.

2. Results & discussion

2.1. Chemistry

The designed compounds were synthesized as depicted in Scheme 1. Substituted pyridin-2-amines reacted with 1,1-dimethoxy-*N,N*-dimethylmethanamine in methanol at 70 °C to yield *N,N*-dimethyl-*N'*-(pyridin-2-yl)formimidamide derivatives **2a-d**.⁸ Substituted 2-chloro-1-(imidazo[1,2-*a*]pyridin-3-yl)ethanone **3a-d** were synthesized from **2a-d** using 1,3-dichloropropan-2-one in acetonitrile at room temperature as described in Scheme 1.^{8,14} Reaction of imidamide derivatives **4a-c** in presence of (isothiocyanatomethanetryl)tribenzene in THF at 50 °C for 3–4 h afforded substituted *N'*-(tritylcarbamothioyl)formimidamides **5a-c**.¹⁵ Thiourea **6** reacted with 1,1-dimethoxy-*N,N*-dimethylmethanamine to afford *N'*-carbamothioyl-*N,N*-dimethylformimidamide **7**. **7** was reacted in presence of (isothiocyanatomethanetryl) tribenzene in THF at 50 °C for 3–4 h to yield *N,N*-dimethyl-*N'*-(tritylcarbamothioyl) formimidamide **8**.¹⁶ Substituted 2-chloro-1-(imidazo[1,2-*a*]pyridin-3-yl) ethanones **3a-d** were reacted with substituted *N'*-(tritylcarbamothioyl) formimidamides **5a-c** and **8** to yield **9a-p**. **9a-p** were further reacted for the deprotection of trityl group by trifluoro acetic acid to get the final compounds, substituted (2-aminothiazol-5-yl)(imidazo[1,2-*a*]pyridin-3-yl)methanones **10a-p** (refer Table 1 for specific substitutions). All the synthesized compounds were purified by column chromatography and purity of the compounds was checked by HPLC chromatogram. Further, compounds were characterized by ¹H NMR and ¹³C NMR spectra (See supplementary material for spectral data).

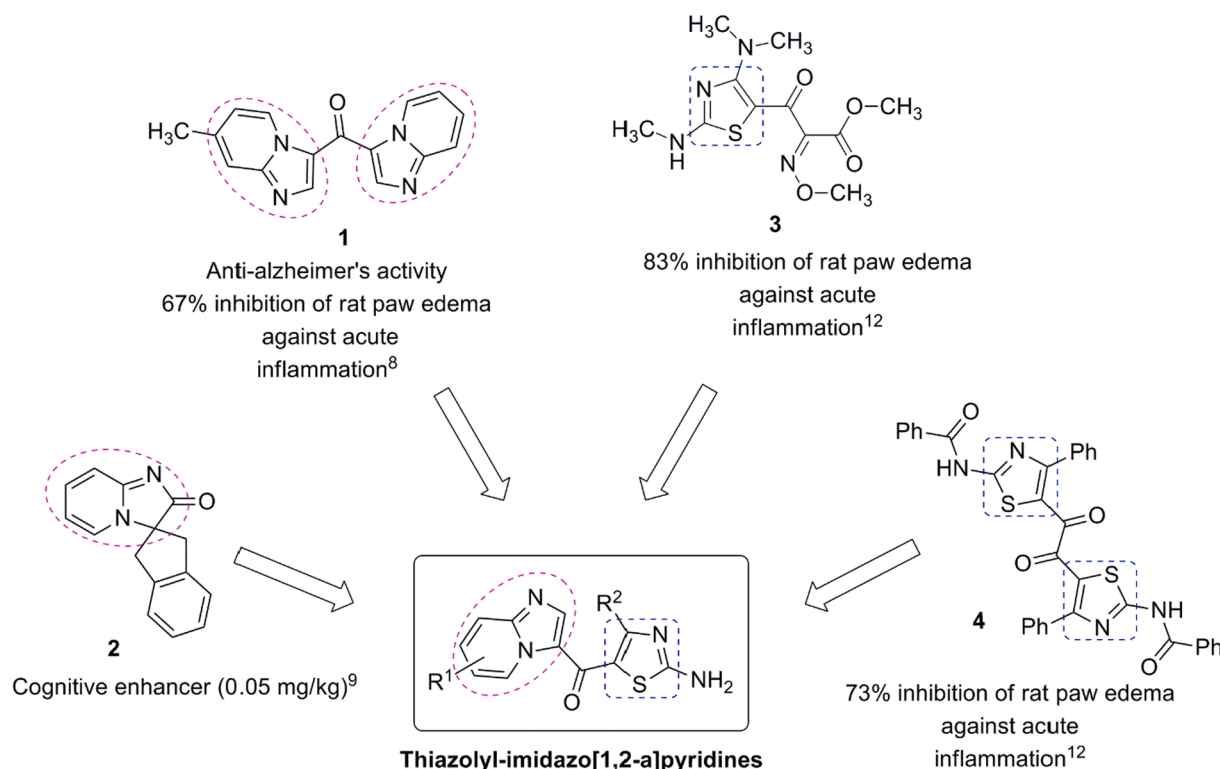
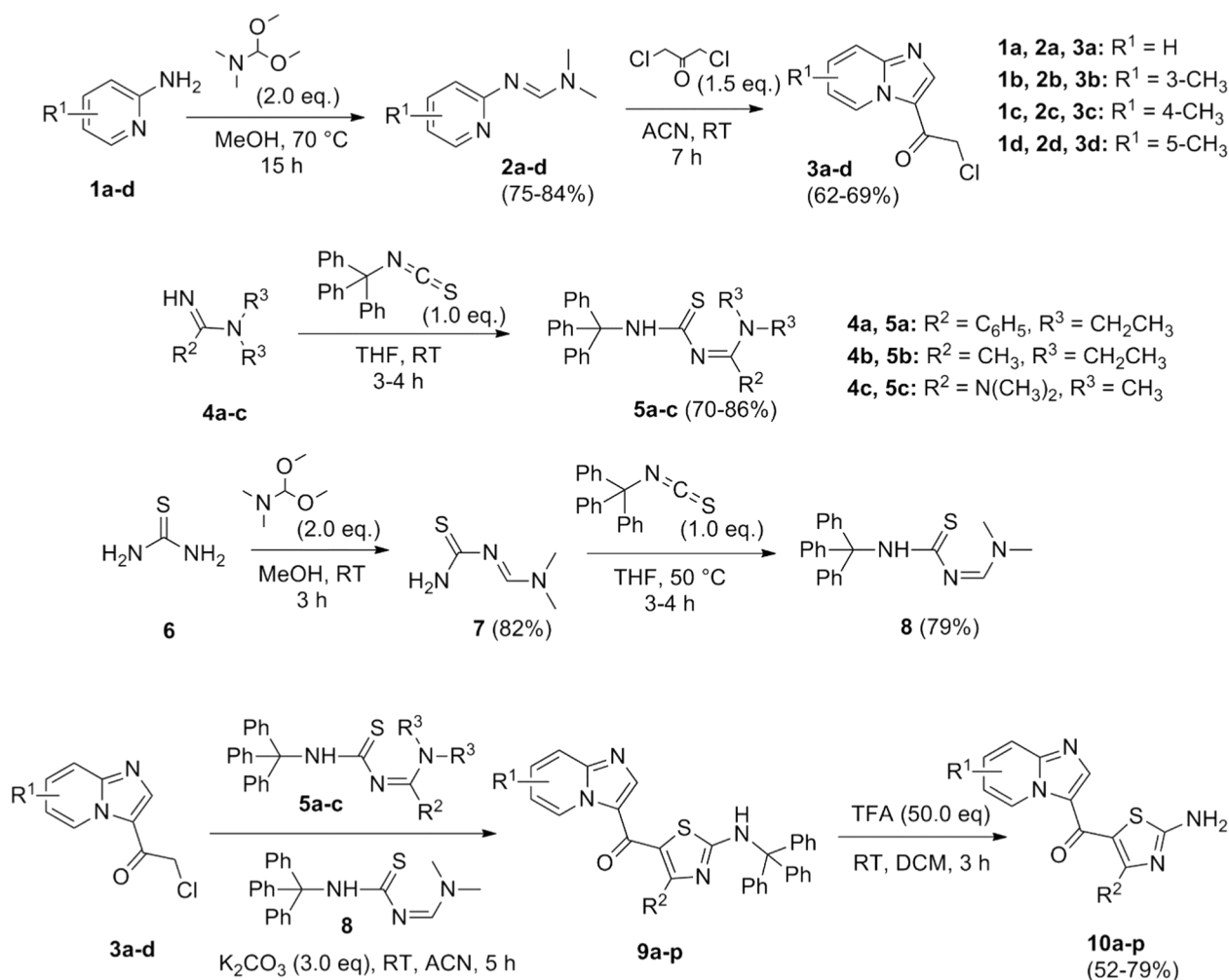


Fig. 1. Design of thiazolyl-imidazo[1,2-*a*]pyridines.



Scheme 1. Synthesis of thiazolyl-imidazo[1,2-a]pyridine derivatives.

2.2. In vivo acute inflammation study

The anti-inflammatory potential of the compounds **10a-p** were tested by studying acute and chronic inflammation model. All the compounds were examined using carrageenan induced acute inflammation rat model. Carrageenan was given subcutaneously to the left hind paw of each rat. This causes metabolism of arachidonic acid and further produces plasma and leukocyte extravasations, plasma protein exudation along with neutrophil extravasations and increased tissue water. This inflammatory event was diminished by our compounds at $50 \text{ mg}\cdot\text{kg}^{-1}$ dose. % decrease in the size of edema was calculated and reported as % edema inhibition in Table 1. During carrageenan induced acute inflammation, COX-1 and COX-2 both the enzymes are involved in the inflammatory event. Therefore, non-selective COX inhibitor, Diclofenac was used as a standard drug.¹⁷⁻¹⁹ Data expressed as mean \pm SEM. Test compounds were compared with the standard drug diclofenac (dose of $7.5 \text{ mg}\cdot\text{kg}^{-1}$). Compounds **10b**, **10c**, **10h**, **10i**, **10k**, **10o** and **10p** were found to inhibit inflamed paw with % inhibition of 81%, 85%, 77%, 53%, 66%, 77%, and 53%, respectively. Standard drug, diclofenac was found to inhibit rat paw edema with 72%.

2.3. In vivo chronic inflammation study

Active compounds from the acute inflammation study, i.e. **10b**, **10c** and **10o** were taken further to evaluate their anti-inflammatory activity using formalin induced chronic inflammation model. Compounds **10b** and **10c** were found to show anti-inflammatory activity during 5 days of

chronic inflammation model. On 5th day of chronic model, % inhibition of edema was obtained as 54% and 63% for **10b** and **10c**, respectively. Celecoxib (selective COX-2 inhibitor) was used as a standard drug because COX-2 is a major contributor to prostanoid synthesis in chronic phase of inflammation.¹⁷⁻¹⁹ Celecoxib was found to inhibit 68% of rat paw edema as given in Table 2.

Compound **10c** had shown both acute as well as chronic anti-inflammatory activities, so it was taken further to evaluate its activity in AlCl_3 induced Alzheimer's disease model. During the 28 days of Alzheimer's disease model, various behavioral parameters, biochemical parameters and haematological parameters were assessed. Meloxicam was taken as a standard drug for AlCl_3 induced (AD) model because it protects neurons by reducing metal ion imbalance induced oxidative stress.²⁰

2.4. AlCl_3 induced Alzheimer's disease (AD) model

2.4.1. Estimation of behavioral parameters

2.4.1.1. Evaluation of transfer latency by elevated plus maze test. Spatial working memory of the rats was evaluated using elevated plus maze test. It is a natural tendency of rats to escape from the elevated open space environment and to be in the close and safe environment. Transfer latency (TL) measures this behavior of rats. Time required for each rat to reach to the closed arm from an open arm was measured (in seconds).²¹ Treatment with compound **10c** improved the spatial working memory of rats when compared to DC rats as shown in Fig. 2A. Memory enhancing

Table 1

List of synthesized compounds with % inhibition of edema in acute inflammation model.

Code	10a ^a p		% inhibition of edema [mean ± SEM] ^a
	R ¹	R ²	
10a	H	N(CH ₃) ₂	32 ± 1.0
10b	3-CH ₃	N(CH ₃) ₂	81 ± 1.5
10c	4-CH ₃	N(CH ₃) ₂	85 ± 0.9
10d	5-CH ₃	N(CH ₃) ₂	23 ± 2.1
10e	H	C ₆ H ₅	40 ± 3.5
10f	3-CH ₃	C ₆ H ₅	20 ± 2.5
10g	4-CH ₃	C ₆ H ₅	26 ± 3.9
10h	5-CH ₃	C ₆ H ₅	77 ± 1.5
10i	H	CH ₃	53 ± 1.2
10j	3-CH ₃	CH ₃	45 ± 1.8
10k	4-CH ₃	CH ₃	66 ± 1.1
10l	5-CH ₃	CH ₃	33 ± 2.4
10m	H	H	33 ± 2.6
10n	3-CH ₃	H	31 ± 2.4
10o	4-CH ₃	H	77 ± 0.8
10p	5-CH ₃	H	53 ± 1.0
Diclofenac	—	—	72 ± 1.3

^a Data expressed as the % inhibition in edema size relative to the DC group. Statistical analysis was performed by One-way ANOVA followed by Tukey's multiple comparison test. Mean ± SEM (n = 6 rats/group) *p < 0.05.

Table 2

% edema inhibition against formalin induced chronic inflammation.

Compound	% Inhibition of edema in chronic inflammation [mean ± SEM] ^a				
	Day 1	Day 2	Day 3	Day 4	Day 5
10b	55 ± 3.3	56 ± 2.0	56 ± 1.0	54 ± 3.7	54 ± 3.9
10c	58 ± 3.2	67 ± 3.0	65 ± 3.9	60 ± 4.7	63 ± 3.8
10o	30 ± 1.6	24 ± 2.3	36 ± 4.7	23 ± 1.0	18 ± 4.9
Celecoxib	67 ± 1.8	74 ± 1.1	70 ± 4.4	70 ± 2.9	68 ± 1.0

^a Data expressed as the % inhibition in edema size relative to the DC group. Statistical analysis was performed by One-way ANOVA followed by Tukey's multiple comparison test. Mean ± SEM (n = 6 rats/group) *p < 0.05.

effect of compound 10c was evaluated during 7th, 14th, 21st and 28th day of AlCl₃ induced AD model.

2.4.1.2. Evaluation of conditioned avoidance response using pole climbing apparatus. Conditioned avoidance response (CAR) was evaluated using pole climbing apparatus. This test demonstrates learning memory of rats.²² During acquisition session, rats showed low CAR values as they learned to escape from the foot shock. Whereas during test session, DC rats showed significantly high CAR values on 7th, 14th, 21st and 28th day of AlCl₃ model. Learning memory of rats were improved when treated with the compound 10c when compared with DC group rats ([#]p < 0.05) as depicted in Fig. 2B.

2.4.1.3. Evaluation of simultaneous alteration performance using Y maze apparatus. Simultaneous alteration performance was assessed by using Y maze apparatus. This test uses the natural tendency of rats to explore new environment, so rats were preferred to visit different maze then previously visited maze.²³ Immediate working memory of rats was monitored by calculating % alteration of all the groups as shown in Fig. 2C. Treatment with 10c significantly improves the working memory when compared with the DC group rats ([#]p < 0.05).

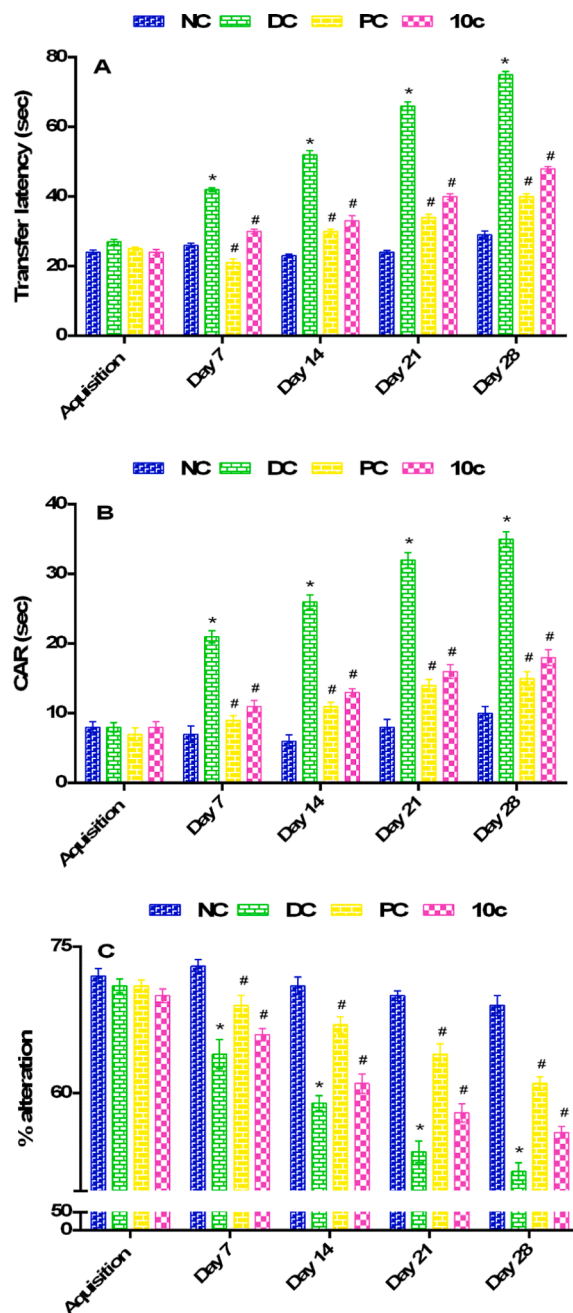


Fig. 2. Behavioral parameters estimation. (A) Results of transfer latency using elevated plus maze test. (B) Results of conditioned avoidance response (CAR) using pole climbing apparatus (C) Results of Y maze test expressed as % alteration. Data expressed as mean ± SEM. Asterisk denotes statistical significance (*p < 0.05) when compared to NC group and ([#]p < 0.05) when compared to DC group, using two-way ANOVA followed by Tukey's multiple comparison test.

2.4.2. Haematological parameters estimation

On 29th day of AlCl₃ model, rats were sacrificed and various haematological parameters, biochemical parameters and anti-oxidant properties were measured using brain tissues. Haemoglobin (HGB) and haematocrit (HCT) level were estimated on the 29th day of AlCl₃ model. HGB and HCT level were significantly reduced in the PC animals compared to NC animals. Whereas, 10c treated rats showed no difference in the HGB and HCT level in blood samples as shown in Fig. 3A and 3B. Reduction in HGB and HCT level in PC animals is due to the gastric injury and bleeding, which was further confirmed in gastrointestinal

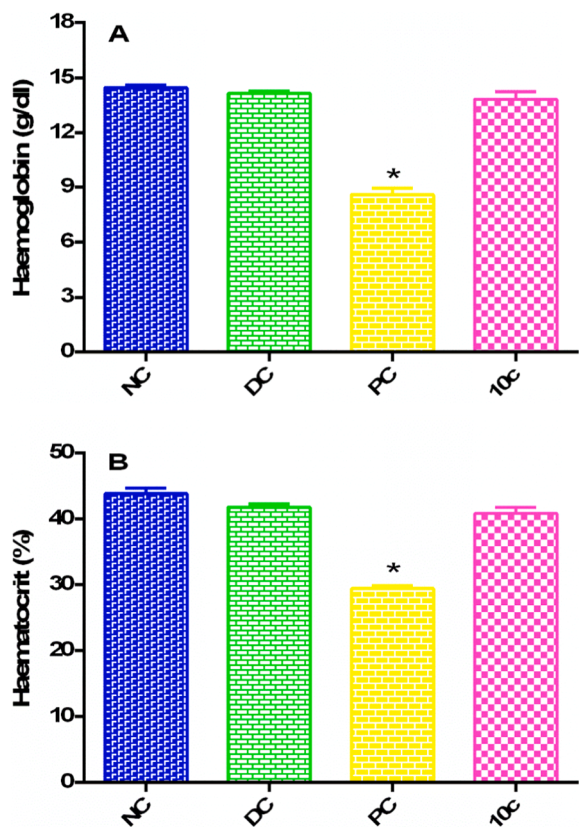


Fig. 3. Estimation of haematological parameters. (A) HGB level was significantly decreased in the PC animals. Data presented as mean \pm SEM ($*p < 0.05$). (B) HCT level estimation in all the groups indicated that there was a significant reduction in the HCT level in PC group when compared to all the groups. Data expressed as mean \pm SEM ($*p < 0.05$) by using 1 way ANOVA followed by Tukey's multiple comparison test.

safety studies.

2.4.3. Biochemical parameters estimation

Serum biochemical parameters viz. serum albumin and total protein were measured in all groups of animals. There was no significant difference in the serum albumin level of all the groups of animals. However, the PC group showed significant decrease in the total protein level as compared to NC animals ($*p < 0.05$) (Fig. 4).

2.4.4. Antioxidant activity

$AlCl_3$ is responsible for the cell damage via free radical generation. This causes increase in the oxidative stress in brain. These free radicals mediate increase in the peroxidase level, which was evaluated by lipid peroxidation assay (LPO).⁸ Antioxidant property of the **10c** was evaluated by superoxide dismutase assay (SOD) of brain tissues. Fig. 5 shows LPO and SOD activity of brain tissues in different groups of rats. LPO activity was measured as formation of MDA level. LPO activity was expressed as [(nmol/gm fresh weight) $\times 10^{-5}$]. $AlCl_3$ treated group significantly increased MDA level when compared to NC animals ($*p < 0.05$). Treatment with **10c** reduces the LPO activity and showed comparable results with PC rats as shown in Fig. 5A. In case of SOD, significant change ($*p < 0.05$) was observed in PC animals and **10c** treated rats when compared with DC rats. Significant change in SOD values were also observed between NC and DC animals ($*p < 0.05$). Normal defense mechanism of body causes slight increase in the SOD level in DC group animals as shown in Fig. 5B.

2.4.5. Neuroprotective effects of compound 10c

Brain sections were stained with HE stain and hippocampal regions

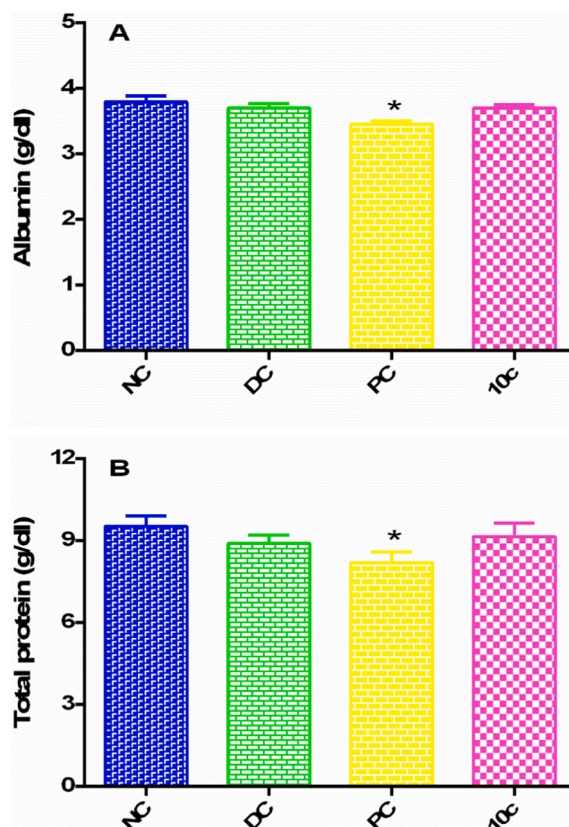


Fig. 4. Estimation of biochemical parameters. (A) Serum albumin level estimation. Data presented as mean \pm SEM ($*p < 0.05$). (B) Total protein estimation. Data expressed as mean \pm SEM ($*p < 0.05$) by using 1 way ANOVA followed by Tukey's multiple comparison test.

of all the groups of rats were observed under 100X magnified microscope. Hippocampal neuronal degeneration is observed in the DC rats. Notably, NC, PC and **10c** treated animals had shown intact neuronal cells. **10c** treated rats had shown the neuro-protective effects comparable with that of PC rats (Fig. 6).

2.4.6. Anti-amyloid properties of compound 10c

Determination of amyloid plaque formation was done by congo red stain. Effect of compound **10c** was observed against amyloid plaques. DC group rats had amyloid plaques in their brain and treatment with **10c** reduces the plaque formation in the cortex region of brain as shown in Fig. 7.

2.5. Determination of gastrointestinal damage

Macroscopic evaluation of gastrointestinal tract was carried out on the 29th day of $AlCl_3$ model. Damage of gastrointestinal tract was measured by using Vernier calipers. Stomach and intestines were observed for lesion indices. PC group rats showed damage in both stomach and intestines. Lesion index in stomach was found to be 12.19 ± 0.8 mm and 29.15 ± 1.6 mm for intestines as shown in Fig. 8. Compound **10c** treated animals had not shown any lesions in the stomach and intestines. Despite being an anti-inflammatory compound, **10c** had no gastrointestinal damaging effect when compared with other NSAIDs.^{24,25}

2.5.1. Histopathological evaluation of gastrointestinal damage

Damage of gastrointestinal track was further checked by microscopic evaluation of stomach and intestinal sections. Sections were stained with HE stain and gastric injuries were confirmed in PC treated animals.

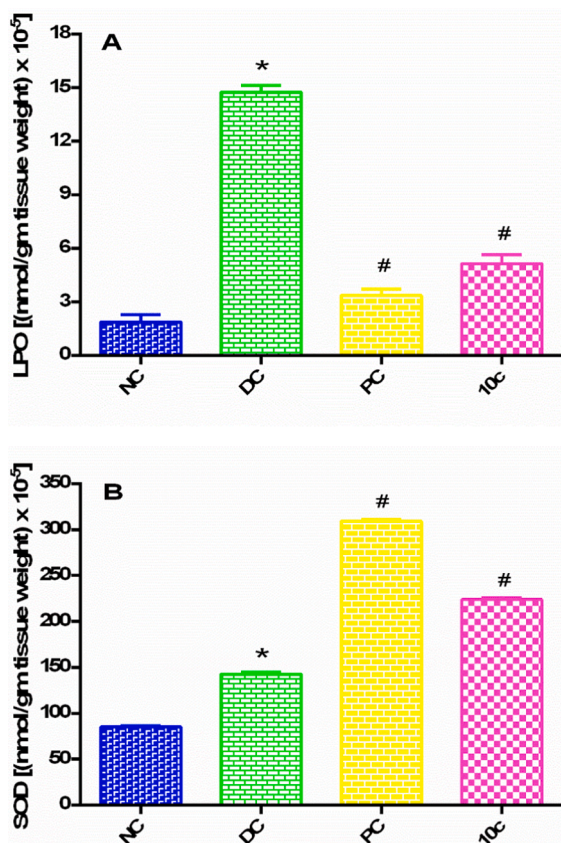


Fig. 5. Anti-oxidative effect of compound 10c. (A) Lipid peroxidation (LPO) expressed as MDA level in rat brain homogenate (B) Super oxide dismutase activity in rat brain homogenate. Data shown as mean \pm SEM (n = 6 rats/group) *p < 0.05 when compared with NC group and #p < 0.05 when compared to DC group using 1 way ANOVA followed by Tukey's multiple comparison test.

PC treated rats had focal erosions present in the stomach and epithelium damage was seen in the intestinal sections. Compound 10c treated animals revealed no erosions in stomach and intestine as shown in Fig. 9 and Fig. 10.

3. Conclusion

There are several factors that affect the AD aetiology. One of the major factors that influences AD progression are neuronal cell inflammation. Damaged neurons and amyloid plaques release several inflammatory cytokines namely TNF- α , IL-1 β and COXs. This inflammatory event lead to neuronal cell degeneration and cell death. Hence to combat AD, treatment with anti-inflammatory leads can serve as a therapeutic weapon. Imidazo[1,2-a]pyridines and thiazoles were fused in a single molecule to make thiazolyl-imidazo[1,2-a]pyridines in order to enhance the anti-inflammatory potency of this fused scaffold. A series of 16 compounds were synthesized and characterized by spectral data. Further, these molecules were tested for their anti-inflammatory benefits using *in vivo* acute and chronic inflammation model. Overall, compound 10c exhibited promising anti-inflammatory activity. Compound 10c was further evaluated for anti-Alzheimer's activity using *in vivo* AlCl₃ induced model. In this study, 10c showed promising results by exhibiting anti-amnesic, neuroprotective and anti-amyloid activities. Furthermore, compound 10c did not exhibit GI toxicity like other NSAIDs. In future, compound 10c may emerge as a promising lead candidate for the treatment of AD.

4. Experimental section

4.1. General methods

Unless stated otherwise solvents and reagents were purchased from commercial suppliers and used without further purification. Determination of melting point was done by using scientific melting point apparatus (Veego; Model VMP-DS) and uncorrected. FTIR spectra were recorded using Shimadzu's IR Affinity 1 apparatus. ¹H NMR and ¹³C NMR spectra were recorded using Bruker Avance II NMR spectrophotometer at frequencies 400 MHz & 100 MHz, respectively. Chemical shift values are represented in parts per million. Signals are described as s (singlet), d (doublet), t (triplet), q (quartet), m (multiplet) and dd (doublet of doublets). LC-ESI-MS spectral data were obtained using Perkin Elmer mass spectrometer. Q-TOF micromass (ESI-MS) was used for HRMS spectral analysis. Pre-coated TLC plates were used for reaction monitoring (Merck). Visualization of TLC plates was done using UV chamber. SHIMADZU-LC-2010 HPLC was used for determination of purity of the compounds. Paw volumes were recorded using manual mercury plethysmometer. Samples were homogenized using Polytron homogenizer (Kinematica, Switzerland). Sorvall Legend X1R centrifuge (Thermo Scientific) was used for Centrifugation. Samples were vortexed in Vortex Mixer (Etek, VM301). Shimadzu UV/Visible Spectrophotometer UV-1800 was used for absorbance of samples. Serum albumin and total protein were determined using fully automated random access clinical chemistry analyser Transasia EM 360. VetScan HM-5 was used for Haemoglobin and haematocrit level estimation. Histopathological slides were observed under optical microscope ProgRes C3 OLYMPUS, U-TV1 X, Japan.

4.2. Chemistry

4.2.1. Synthesis and characterization of substituted *N,N*-dimethyl-*N'*-(pyridin-2-yl)formimidamide (2a-d)

4.2.1.1. *N,N*-dimethyl-*N'*-(pyridin-2-yl)formimidamide (2a). To the solution of pyridin-2-amine (1.0 eq.) in methanol, 1,1-dimethoxy-*N,N*-dimethylmethanamine (2.0 eq.) was added drop wise. Reaction was allowed to proceed at 70 °C for 15 h. After completion of reaction, methanol was evaporated *in vacuo* and concentrated reaction mixture was poured into ice cold water. The product was extracted by dichloromethane (3 × 50 mL). The organic layers were combined, dried over sodium sulfate and evaporated *in vacuo* to get yellow liquid *N,N*-dimethyl-*N'*-(pyridin-2-yl)formimidamide (2a).^{8,14} Yield: 81%; Boiling point: 101–103 °C; LC-ESI-MS (*m/z*): 150.09 [M+H]⁺.

4.2.1.2. *N,N*-dimethyl-*N'*-(3-methylpyridin-2-yl)formimidamide (2b). Intermediate 2b was prepared by the procedure described in 2a using 3-methylpyridin-2-amine. Yield: 75%; Yellow solid; Melting point: 50–52 °C; LC-ESI-MS (*m/z*): 164.1 [M+H]⁺.

4.2.1.3. *N,N*-dimethyl-*N'*-(4-methylpyridin-2-yl)formimidamide (2c). Intermediate 2c was prepared by the procedure described in 2a using 4-methylpyridin-2-amine. Yield: 84%; Yellow solid; Melting point: 55–57 °C; LC-ESI-MS (*m/z*): 164.2 [M+H]⁺.

4.2.1.4. *N,N*-dimethyl-*N'*-(5-methylpyridin-2-yl)formimidamide (2d). Intermediate 2d was prepared by the procedure described in 2a using 5-methylpyridin-2-amine. Yield: 77%; Yellow solid; Melting point: 53–55 °C; LC-ESI-MS (*m/z*): 164.1 [M+H]⁺.

4.2.2. Synthesis and characterization of substituted 2-chloro-1-(imidazo[1,2-a]pyridin-3-yl)ethanone (3a-d)

4.2.2.1. 2-chloro-1-(imidazo[1,2-a]pyridin-3-yl)ethanone (3a). To the

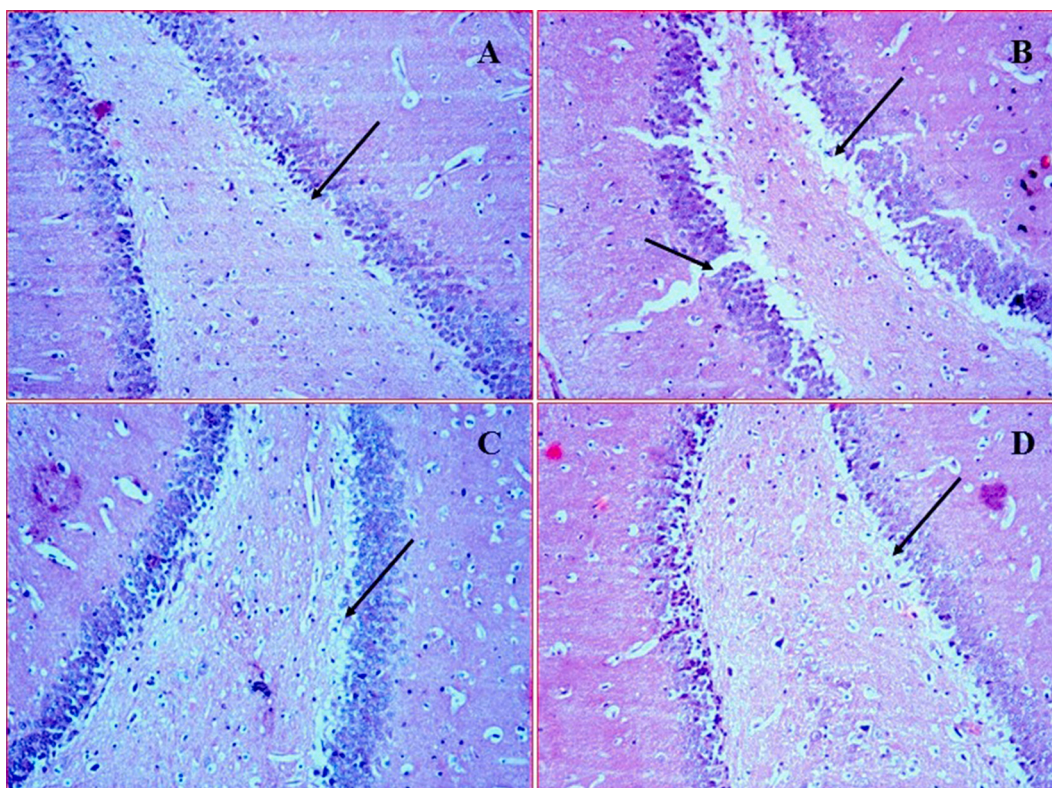


Fig. 6. Typical microscopic HE stained sections (under 100X magnification) of brain hippocampus (A) NC animals had shown normal and healthy hippocampal neurons (B) DC animals had shown degenerated neuronal cells in hippocampus (C) PC animals showed healthy neurons in hippocampus, (D) 10c treated rats showed healthy neuronal cells.

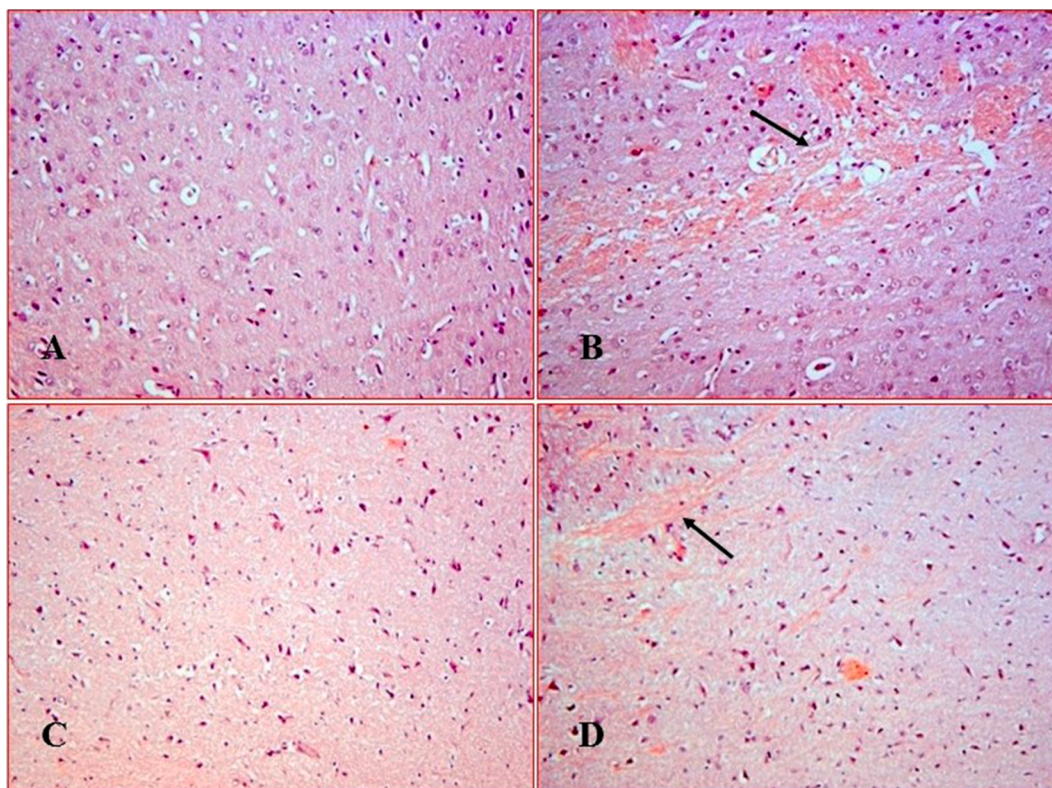


Fig. 7. Congo red stained sections (under 100X magnification) of brain cortex in all the groups. (A) NC animal's brain cortex without amyloid plaques (B) Amyloid plaques were present in the cortex of DC rats (stained red) indicated by an arrow, (C) PC animals without plaques (D) Reduction in the amyloid plaque by treatment with compound 10c as indicated by an arrow.

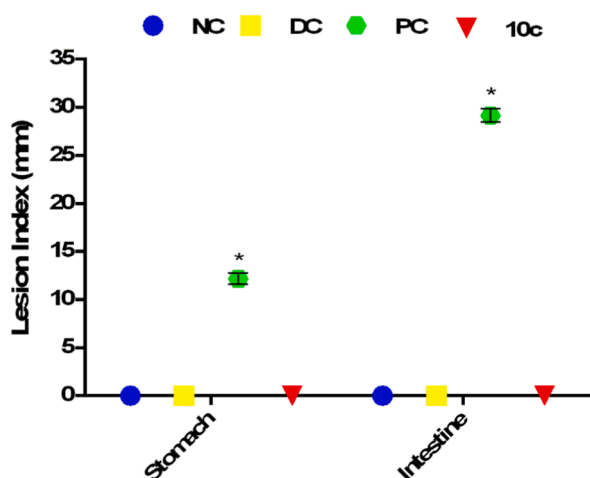


Fig. 8. Determination of lesion index: PC group animals showed significantly higher lesion index when compared to NC, DC and 10c treated groups. Data expressed as mean \pm SEM (* $p < 0.05$) by using 1 way ANOVA followed by Tukey's multiple comparison test.

solution of 1,3-dichloropropan-2-one (1.5 eq.) in acetonitrile, *N,N*-dimethyl-*N'*-(pyridin-2-yl)formimidamide (1.0 eq.) was added drop wise. Reaction mixture was allowed to stir at room temperature for 7 h. After completion of reaction, reaction mixture was poured into ice cold water to obtain crude brown solid of **3a**. Resulting crude was crystallized in methanol to get pure 2-chloro-1-(imidazo[1,2-*a*]pyridin-3-yl)ethanone (**3a**).¹⁴ Yield: 62%; White solid; Melting point: 138–140 °C; LC-ESI-MS (m/z): 195.5 [M+H]⁺.

4.2.2.2. 2-chloro-1-(8-methylimidazo[1,2-*a*]pyridin-3-yl)ethanone (**3b**). Intermediate **3b** was prepared by the procedure described in **3a** using *N*,

N-dimethyl-*N'*-(3-methylpyridin-2-yl)formimidamide. Yield: 68%; Colorless solid; Melting point: 135–137 °C; LC-ESI-MS (m/z): 209.5 [M+H]⁺.

4.2.2.3. 2-chloro-1-(7-methylimidazo[1,2-*a*]pyridin-3-yl)ethanone (**3c**). Intermediate **3c** was prepared by the procedure described in **3a** using *N,N*-dimethyl-*N'*-(4-methylpyridin-2-yl)formimidamide. Yield: 69%; Pale yellow solid, Melting point: 134–136 °C; LC-ESI-MS (m/z): 209.5 [M+H]⁺.

4.2.2.4. 2-chloro-1-(6-methylimidazo[1,2-*a*]pyridin-3-yl)ethanone (**3d**). Intermediate **3d** was prepared by the procedure described in **3a** using *N,N*-dimethyl-*N'*-(5-methylpyridin-2-yl)formimidamide. Yield: 64%; Colorless solid, Melting point: 135–137 °C; LC-ESI-MS (m/z): 209.5 [M+H]⁺.

4.2.3. Synthesis and characterization of substituted *N'*-(tritylcarbamothioyl) formimidamides (**5a-c**)

4.2.3.1. *N,N*-diethyl-*N'*-(tritylcarbamothioyl)benzimidamide (**5a**). To the solution of *N,N*-diethylbenzimidamide **4a** (1.0 eq.) in THF, addition of (isothiocyanatomethanetryl)tribenzene (1.0 eq.) was done. Reaction mixture was allowed to stir at room temperature for 3–4 h. After completion of reaction, THF was evaporated *in vacuo* to get colorless solid of **5a**.¹⁵ The crude was purified by column chromatography (1:9 = Ethyl acetate: Hexane). Yield: 82%; colorless solid; Melting point: 195–197 °C; LC-ESI-MS (m/z): 478.1 [M+H]⁺.

4.2.3.2. *N,N*-diethyl-*N'*-(tritylcarbamothioyl)acetimidamide (**5b**). Intermediate **5b** was prepared by the procedure described in **5a** using *N,N*-diethylacetimidamide. Yield: 70%; Melting point: 188–190 °C; LC-ESI-MS (m/z): 416.2 [M+H]⁺.

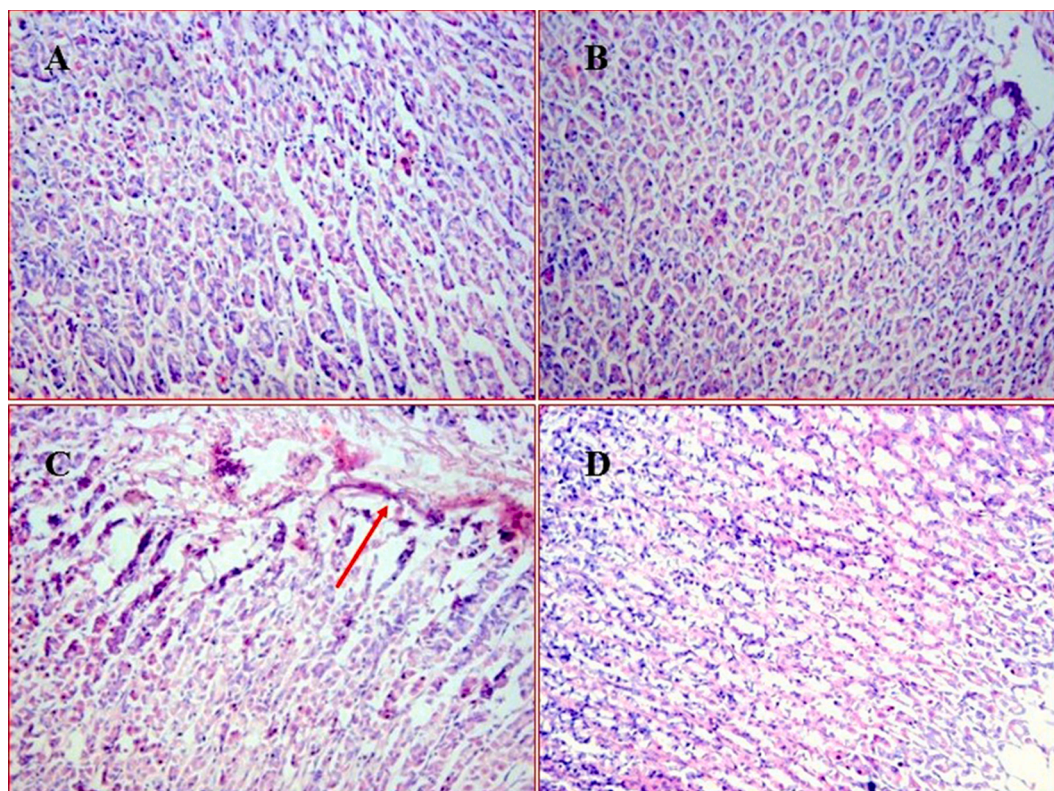


Fig. 9. Typical microscopic HE stained sections (under 100X magnification) of stomach in all the groups. (A) NC animals without stomach erosions, (B) DC animals without erosions, (C) PC animals with focal erosions indicated by an arrow, (D) Absence of ulceration and erosions in 10c treated animals.

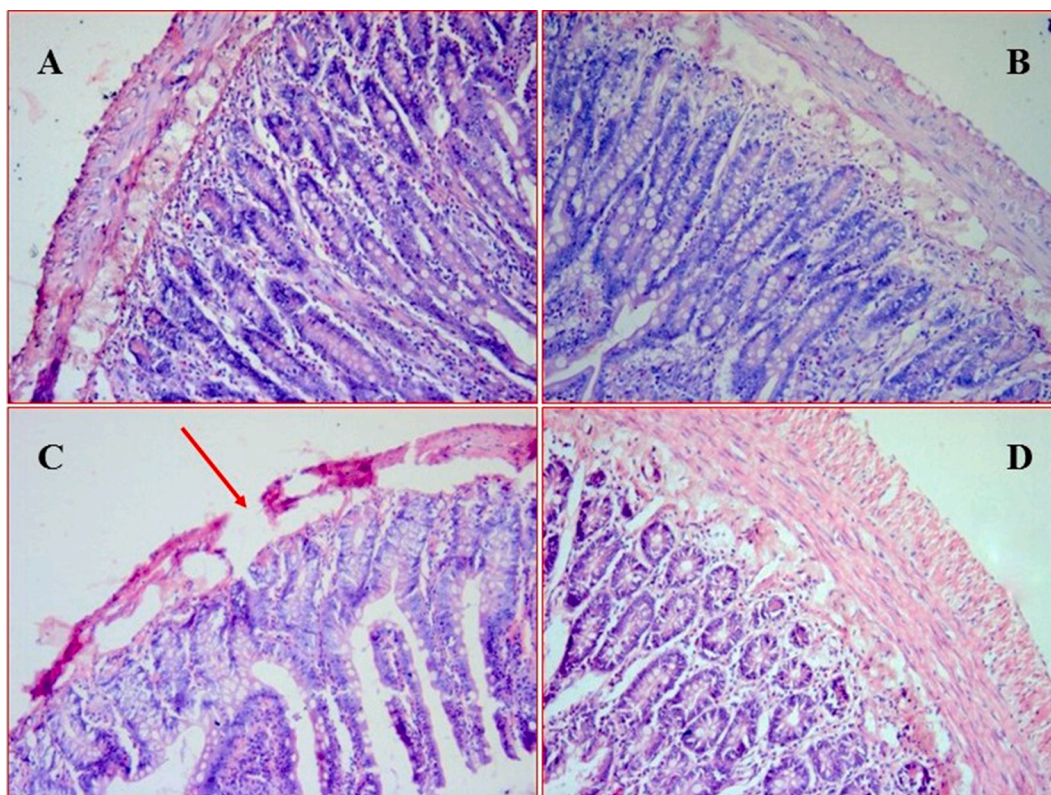


Fig. 10. Typical microscopic HE stained sections (under 100X magnification) of intestine in all the groups. (A) NC animals did not show any ulceration (B) DC animals without any focal erosions, (C) PC animals showed focal erosions of the superficial epithelium and epithelial stratification indicated by an arrow, (D) No erosions or epithelium stratification was observed in 10c treated animals.

4.2.3.3. 1-(bis(dimethylamino)methylene)-3-tritylthiourea (5c). Intermediate **5c** was prepared by the procedure described in **5a** using 1,1,3,3-tetramethylguanidine. Yield: 86%; Melting point: 182–184 °C; LC-ESI-MS (m/z): 417.2 [M+H]⁺.

4.2.4. Synthesis and characterization of *N,N*-dimethyl-*N'*-(tritylcarbamothioyl)formimidamide (8)

Thiourea **6** (1.0 eq) in methanol was reacted with 1,1-dimethoxy-*N,N*-dimethylmethanamine (2.0 eq) at room temperature for 3 h to get *N'*-carbamothioyl-*N,N*-dimethylformimidamide **7** (yield 82%). **7** (1.0 eq) was further reacted with (isothiocyanatomethanetryl)tribenzene in THF, at 50 °C for 3–4 h to yield intermediate **8**. After completion of reaction, THF was evaporated *in vacuo* to get compound **8**.¹⁶ **8** was purified by column chromatography (1:9 = Ethyl acetate: Hexane). Yield: 79%; Pale yellow solid; Melting point: 210–212 °C; LC-ESI-MS (m/z): 374.1 [M+H]⁺.

4.2.5. Synthesis and characterization of final compounds: Substituted (2-aminothiazol-5-yl)(imidazo[1,2-*a*]pyridin-3-yl)methanones (10a-p)

4.2.5.1. (2-amino-4-(dimethylamino)thiazol-5-yl)(imidazo[1,2-*a*]pyridin-3-yl)methanone (10a). To a solution of 2-chloro-1-(imidazo[1,2-*a*]pyridin-3-yl)ethanone (1.0 eq.) **3a** in acetonitrile, K₂CO₃ (3.0 eq.) was added. Reaction mixture was allowed to stir and addition of 1-(bis(dimethylamino)methylene)-3-tritylthiourea (1.0 eq.) **5c** was done slowly. Reaction was allowed to stir at room temperature for 5 h. After completion of reaction, reaction mixture was poured into ice cold water to get the precipitates of tritylated **9a**. Deprotection of tritylated **9a** was done using trifluoro acetic acid (50.0 eq.) in DCM for 3 h. After completion of reaction, reaction mixture was poured into ice cold water. Solution was neutralized with sodium bicarbonate to get the product **10a**. **10a** was purified by column chromatography (Chloroform:

Methanol = 9.5:0.5). SHIMADZU-LC-2010 was used to determine the purity of each compound [Mobile phase (10 mM):- KH₂PO₄ buffer: Acetonitrile (50:50); Column: Reverse phase; pH: 7]. Pale yellow solid; Yield: 76%; Purity: 99.1%; Melting point: 180–182 °C; Molecular formula: C₁₃H₁₃N₅OS; LC-ESI-MS (m/z): 288.1 [M+H]⁺; IR (KBr, cm⁻¹): 3391.23, 3305.25, 3056.21, 1643.52; ¹H NMR (400 MHz, DMSO-*d*₆) δ: 3.05 (s, 6H), 7.045 (t, *J* = 5.6 Hz, 2H), 7.352 (s, 1H), 7.90 (d, *J* = 6.5 Hz, 2H), 8.2114 (s, D₂O exchangeable, 2H); ¹³C NMR (100 MHz, DMSO-*d*₆) δ: 40.1 (2C), 115.50, 117.28, 127.76, 128.03, 128.28, 129.03, 130.40, 139.87, 140.81, 151.24, 164.12.

4.2.5.2. (2-amino-4-(dimethylamino)thiazol-5-yl)(8-methylimidazo[1,2-*a*]pyridin-3-yl)methanone (10b). Final compound **10b** was synthesized as per the procedure described in **10a** using starting materials 2-chloro-1-(8-methylimidazo[1,2-*a*]pyridin-3-yl)ethanone **3b** and 1-(bis(dimethylamino)methylene)-3-tritylthiourea **5c**. **10b** was purified by column chromatography (Chloroform: Methanol = 9.7:0.3). Pale yellow solid; Yield: 71%; Purity: 99.6%; Melting point: 170–172 °C; Molecular formula: C₁₄H₁₅N₅OS; LC-ESI-MS (m/z): 302.09 [M+H]⁺; HRMS (TOF) m/z calcd for C₁₄H₁₅N₅OS [M+H]⁺ 302.3668, found: 302.3623; IR (KBr, cm⁻¹): 3471.87, 3313.71, 3084, 1681.93; ¹H NMR (400 MHz, DMSO-*d*₆) δ: 2.51 (s, 3H), 3.02 (s, 6H), 6.99 (t, *J* = 6.8 Hz, 1H), 7.27 (d, *J* = 6.7 Hz, 1H), 7.95 (s, D₂O exchangeable, 2H), 8.08 (s, 1H), 9.17 (d, *J* = 6.6 Hz, 1H); ¹³C NMR (100 MHz, DMSO-*d*₆) δ: 16.43, 112.44, 113.21, 125.57, 125.88, 126.59, 137.92, 138.43, 140.86, 164.31, 169.96, 170.04, 175.37.

4.2.5.3. (2-amino-4-(dimethylamino)thiazol-5-yl)(7-methylimidazo[1,2-*a*]pyridin-3-yl)methanone (10c). Final compound **10c** was synthesized as per the procedure described in **10a** using starting materials 2-chloro-1-(7-methylimidazo[1,2-*a*]pyridin-3-yl)ethanone **3c** and 1-(bis(dimethylamino)methylene)-3-tritylthiourea **5c**. **10c** was purified by column

chromatography (Chloroform: Methanol = 9.7:0.3). Yellow solid; Yield: 68%; Purity: 99.9%; Melting point: 173–175 °C; Molecular formula: $C_{14}H_{15}N_5OS$; LC-ESI-MS (m/z): 302.09 $[M+H]^+$; HRMS (TOF) m/z calcd for $C_{14}H_{15}N_5OS$ $[M+H]^+$ 302.3668, found: 302.3654; IR (KBr, cm^{-1}): 3471.87, 3313.71, 3064.89, 1681.93; 1H NMR (400 MHz, DMSO- d_6) δ : 2.33 (s, 3H), 3.02 (s, 6H), 6.96 (d, $J = 6.8$ Hz, 1H), 7.7 (s, 1H), 7.92 (s, D₂O exchangeable, 2H), 8.02 (s, 1H), 9.2 (d, $J = 7.2$ Hz, 1H); ^{13}C NMR (100 MHz, DMSO- d_6) δ : 20.75, 41.72 (2C), 115.57, 116.14, 126.60, 127.03, 127.50, 138.22, 138.60, 147.06, 147.73, 164.19, 169.88.

4.2.5.4. (2-amino-4-(dimethylamino)thiazol-5-yl)(6-methylimidazo[1,2-a]pyridin-3-yl)methanone (10d). Final compound **10d** was synthesized as per the procedure described in **10a** using starting materials 2-chloro-1-(6-methylimidazo[1,2-a]pyridin-3-yl)ethanone **3d** and 1-(bis(dimethylamino)methylene)-3-tritylthiourea **5c**. **10d** was purified by column chromatography (Chloroform: Methanol = 9.7:0.3). Yellow solid; Yield: 79%; Purity: 99.9%; Melting point: 172–174 °C; Molecular formula: $C_{14}H_{15}N_5OS$; LC-ESI-MS (m/z): 302.1 $[M+H]^+$; IR (KBr, cm^{-1}): 3442.94, 3282.84, 3178.69, 1633.71; 1H NMR (400 MHz, DMSO- d_6) δ : 2.34 (s, 3H), 3.02 (s, 6H), 7.352 (d, $J = 1.6$ Hz, 1H), 7.6285 (d, $J = 9.2$ Hz, 1H), 7.931 (s, D₂O exchangeable, 2H), 8.033 (s, 1H), 9.14 (d, $J = 7.0$ Hz, 1H); ^{13}C NMR (100 MHz, DMSO- d_6) δ : 17.78, 41.72 (2C), 92.69, 116.5, 123.04, 125.07, 125.40, 130.12, 138.31, 145.61, 164.32, 169.93, 170.00.

4.2.5.5. (2-amino-4-phenylthiazol-5-yl)(imidazo[1,2-a]pyridin-3-yl)methanone (10e). Final compound **10e** was synthesized as per the procedure described in **10a** using starting materials 2-chloro-1-(imidazo[1,2-a]pyridin-3-yl)ethanone **3a** and *N,N*-diethyl-*N'*-(tritylcarbamothioyl)benzimidamide **5a**. **10e** was purified by column chromatography (Hexane: Ethyl acetate = 4.5:5.5). Yellow solid; Yield: 67%; Purity: 98.9%; Melting point: 187–189 °C; Molecular formula: $C_{17}H_{12}N_4OS$; LC-ESI-MS (m/z): 321.1 $[M+H]^+$; IR (KBr, cm^{-1}): 3371.57, 3278.99, 3128.54, 1612.49; 1H NMR (400 MHz, DMSO- d_6) δ : 7.234 (t, $J = 7.2$ Hz, 4H), 7.47 (d, $J = 6.8$ Hz, 2H), 7.583 (t, $J = 8$ Hz, 1H), 7.71 (d, $J = 8.8$ Hz, 1H), 7.781 (s, 1H), 7.925 (s, D₂O exchangeable, 2H), 9.37 (d, $J = 6.8$ Hz, 2H); ^{13}C NMR (100 MHz, DMSO- d_6) δ : 113.21, 124.32, 126.61 (2C), 127.34, 128.12, 128.93 (2C), 131.30, 132.75, 134.92 (2C), 151.43 (2C), 152.15, 168.63, 174.54.

4.2.5.6. (2-amino-4-phenylthiazol-5-yl)(8-methylimidazo[1,2-a]pyridin-3-yl)methanone (10f). Final compound **10f** was synthesized as per the procedure described in **10a** using starting materials 2-chloro-1-(8-methylimidazo[1,2-a]pyridin-3-yl)ethanone **3b** and *N,N*-diethyl-*N'*-(tritylcarbamothioyl)benzimidamide **5a**. **10f** was purified by column chromatography (Hexane: Ethyl acetate = 1:1). Pale Yellow solid; Yield: 64%; Purity: 99.4%; Melting point: 176–178 °C; Molecular formula: $C_{18}H_{14}N_4OS$; LC-ESI-MS (m/z): 335.3 $[M+H]^+$; IR (KBr, cm^{-1}): 3378.25, 3262.45, 3048.13, 1618.92; 1H NMR (400 MHz, DMSO- d_6) δ : 2.401 (s, 3H), 7.144–7.485 (m, 8H), 7.910 (d, $J = 5.6$ Hz, 2H), 9.255 (d, $J = 5.2$ Hz, 1H), ^{13}C NMR (100 MHz, DMSO- d_6) δ : 20.22, 113.32, 114.12, 124.42, 126.88, 127.45, 128.14, 129.07, 131.36, 132.46, 135.01, 151.41, 152.36, 156.53, 158.69, 159.15, 171.23, 177.54.

4.2.5.7. (2-amino-4-phenylthiazol-5-yl)(7-methylimidazo[1,2-a]pyridin-3-yl)methanone (10g). Final compound **10g** was synthesized as per the procedure described in **10a** using starting materials 2-chloro-1-(7-methylimidazo[1,2-a]pyridin-3-yl)ethanone **3c** and *N,N*-diethyl-*N'*-(tritylcarbamothioyl)benzimidamide **5a**. **10g** was purified by column chromatography (Hexane: Ethyl acetate = 1:1). Yellow solid; Yield: 55%; Purity: 99.7%; Melting point: 171–173 °C; Molecular formula: $C_{18}H_{14}N_4OS$; LC-ESI-MS (m/z): 335.3 $[M+H]^+$; IR (KBr, cm^{-1}): 3460.30, 3242.55, 3086.11, 1645.28; 1H NMR (400 MHz, DMSO- d_6) δ : 2.349 (s, 3H), 6.422 (d, $J = 5.2$ Hz, 1H), 7.231–7.560 (m, 5H), 7.921 (s, D₂O exchangeable, 2H), 8.342 (d, $J =$ Hz, 2H), 9.37 (d, $J = 6.8$ Hz, 1H);

^{13}C NMR (100 MHz, DMSO- d_6) δ : 20.98, 117.39, 117.98, 118.12, 120.90, 122.49, 127.22, 127.27, 127.66, 128.24, 129.13, 135.19, 140.66, 141.35, 144.37, 148.97, 171.31, 180.27.

4.2.5.8. (2-amino-4-phenylthiazol-5-yl)(6-methylimidazo[1,2-a]pyridin-3-yl)methanone (10h). Final compound **10h** was synthesized as per the procedure described in **10a** using starting materials 2-chloro-1-(6-methylimidazo[1,2-a]pyridin-3-yl)ethanone **3d** and *N,N*-diethyl-*N'*-(tritylcarbamothioyl)benzimidamide **5a**. **10h** was purified by column chromatography (Hexane: Ethyl acetate = 1:1). Yellow solid; Yield: 52%; Purity: 99.9%; Melting point: 175–177 °C; Molecular formula: $C_{18}H_{14}N_4OS$; LC-ESI-MS (m/z): 335.3 $[M+H]^+$; IR (KBr, cm^{-1}): 3362.71, 3287.25, 3078.15, 1646.12; 1H NMR (400 MHz, DMSO- d_6) δ : 2.401 (s, 3H), 7.254–7.312 (m, 5H), 7.47 (d, $J = 8.8$ Hz, 1H), 7.74 (d, $J = 7.2$ Hz, 1H), 8.108 (s, 1H), 8.112 (s, D₂O exchangeable, 2H), 9.301 (s, 1H); ^{13}C NMR (100 MHz, DMSO- d_6) δ : 18.12, 113.62, 115.89, 122.01, 124.50, 125.41, 126.75, 127.03, 127.61, 128.14, 130.92, 140.99, 146.73, 147.52, 148.02, 173.26, 173.42, 178.79.

4.2.5.9. (2-amino-4-methylthiazol-5-yl)(imidazo[1,2-a]pyridin-3-yl)methanone (10i). Final compound **10i** was synthesized as per the procedure described in **10a** using starting materials 2-chloro-1-(imidazo[1,2-a]pyridin-3-yl)ethanone **3a** and *N,N*-diethyl-*N'*-(tritylcarbamothioyl)acetimidamide **5b**. **10i** was purified by column chromatography (Hexane: Ethyl acetate = 2.5:7.5). Colorless solid; Yield: 63%; Purity: 99.4%; Melting point: 183–185 °C; Molecular formula: $C_{12}H_{10}N_4OS$; LC-ESI-MS (m/z): 259.2 $[M+H]^+$; IR (KBr, cm^{-1}): 3483.44, 3238.48, 3091.89, 1654.92; 1H NMR (400 MHz, DMSO- d_6) δ : 2.469 (s, 3H), 7.220–7.297 (m, 2H), 7.599 (s, D₂O exchangeable, 2H), 7.8255 (d, $J = 7.6$ Hz, 1H), 8.362 (s, 1H), 9.4535 (d, $J = 8.4$ Hz, 1H); ^{13}C NMR (100 MHz, DMSO- d_6) δ : 18.60, 114.79 (2C), 117.37, 126.60, 127.49, 127.73, 128.24, 128.97, 141.27, 147.73, 159.22.

4.2.5.10. (2-amino-4-methylthiazol-5-yl)(8-methylimidazo[1,2-a]pyridin-3-yl)methanone (10j). Final compound **10j** was synthesized as per the procedure described in **10a** using starting materials 2-chloro-1-(8-methylimidazo[1,2-a]pyridin-3-yl)ethanone **3b** and *N,N*-diethyl-*N'*-(tritylcarbamothioyl)acetimidamide **5b**. **10j** was purified by column chromatography (Hexane: Ethyl acetate = 3:7). Colorless solid; Yield: 68%; Purity: 99.9%; Melting point: 179–181 °C; Molecular formula: $C_{13}H_{12}N_4OS$; LC-ESI-MS (m/z): 273.3 $[M+H]^+$; HRMS (TOF) m/z calcd for $C_{13}H_{12}N_4OS$ $[M+H]^+$ 273.3256, found: 273.3248; IR (KBr, cm^{-1}): 3284.77, 3046.28, 1691.57; 1H NMR (400 MHz, DMSO- d_6) δ : 2.335 (s, 3H); δ 2.671 (s, 3H); δ 7.145 (t, $J = 5.6$ Hz, 1H); δ 7.432 (d, $J = 6.0$ Hz, 1H); δ 7.906 (s, D₂O exchangeable, 2H); δ 8.338 (s, 1H) δ 9.3 (d, $J = 6.4$ Hz, 1H); ^{13}C NMR (100 MHz, DMSO- d_6) δ : 16.39, 18.60, 114.71, 116.16, 124.54, 125.90, 126.87, 127.54, 140.72, 147.05, 159.13, 170.46, 174.08.

4.2.5.11. (2-amino-4-methylthiazol-5-yl)(7-methylimidazo[1,2-a]pyridin-3-yl)methanone (10k). Final compound **10k** was synthesized as per the procedure described in **10a** using starting materials 2-chloro-1-(7-methylimidazo[1,2-a]pyridin-3-yl)ethanone **3c** and *N,N*-diethyl-*N'*-(tritylcarbamothioyl)acetimidamide **5b**. **10k** was purified by column chromatography (Hexane: Ethyl acetate = 3:7). Pale yellow solid; Yield: 78%; Purity: 99.6%; Melting point: 176–178 °C; Molecular formula: $C_{13}H_{12}N_4OS$; LC-ESI-MS (m/z): 273.3 $[M+H]^+$; IR (KBr, cm^{-1}): 3477.66, 3265.49, 3082.25, 1691.57; 1H NMR (400 MHz, DMSO- d_6) δ : 2.452 (s, 3H), δ 3.318 (s, 3H), δ 7.287 (d, $J = 6.4$ Hz, 1H), δ 7.593 (s, D₂O exchangeable, 2H), δ 7.847 (s, 1H), δ 8.288 (s, 1H), δ 9.3315 (d, $J = 6.8$ Hz, 1H); ^{13}C NMR (100 MHz, DMSO- d_6) δ : 16.51, 19.42, 115.52, 117.33, 131.34, 132.48, 133.12, 135.91, 140.12, 150.52, 156.42, 170.52, 179.61.

4.2.5.12. (2-amino-4-methylthiazol-5-yl)(6-methylimidazo[1,2-a]pyridin-3-yl)methanone (10l). Final compound **10l** was synthesized as per the procedure described in **10a** using starting materials 2-chloro-1-(6-methylimidazo[1,2-a]pyridin-3-yl)ethanone **3d** and *N,N*-diethyl-*N'*-(tritylcarbamothioyl)acetimidamide **5b**. **10l** was purified by column chromatography (Hexane: Ethyl acetate = 3:7). Pale yellow solid; Yield: 59%; Purity: 99.8%; Melting point: 170–172 °C; Molecular formula: C₁₃H₁₂N₄O₂S; LC-ESI-MS (*m/z*): 273.3 [M+H]⁺; IR (KBr, cm⁻¹): 3382.15, 3254.91, 3045.22, 1646.88; ¹H NMR (400 MHz, DMSO-*d*₆): δ 2.384 (s, 3H), δ 2.454 (s, 3H), δ 7.4675 (d, *J* = 9.2 Hz, 1H), δ 7.7165 (d, *J* = 9.2 Hz, 1H), δ 7.877 (s, D₂O exchangeable, 2H), δ 8.299 (s, 1H), δ 9.276 (s, 1H); ¹³C NMR (100 MHz, DMSO-*d*₆): δ 16.42, 18.46, 115.22, 117.34, 123.96, 126.01, 126.92, 127.46, 141.05, 148.42, 160.11, 170.52, 174.16.

4.2.5.13. (2-aminothiazol-5-yl)(imidazo[1,2-a]pyridin-3-yl)methanone (10m). Final compound **10m** was synthesized as per the procedure described in **10a** using starting materials 2-chloro-1-(imidazo[1,2-a]pyridin-3-yl)ethanone **3a** and *N,N*-dimethyl-*N'*-(tritylcarbamothioyl)formimidamide **8**. **10m** was purified by column chromatography (Hexane: Ethyl acetate = 1.5:8.5). Pale yellow solid; Yield: 62%; Purity: 99.1%; Melting point: 190–192 °C; Molecular formula: C₁₁H₈N₄O₂S; LC-ESI-MS (*m/z*): 245.2 [M+H]⁺; IR (KBr, cm⁻¹): 3477.66, 3383.14, 3082.25, 1687.71; ¹H NMR (400 MHz, DMSO-*d*₆): δ 7.222–7.303 (m, 4H); δ 7.598 (s, 1H); δ 8.093 (d, *J* = 12.4 Hz, 1H); δ 8.571 (s, 1H); δ 9.4325 (d, *J* = 5.6 Hz, 1H); ¹³C NMR (100 MHz, DMSO-*d*₆): δ 117.37, 122.21, 126.60, 127.01, 127.49, 127.73, 128.01, 128.87, 141.28, 147.73, 173.71.

4.2.5.14. (2-aminothiazol-5-yl)(8-methylimidazo[1,2-a]pyridin-3-yl)methanone (10n). Final compound **10n** was synthesized as per the procedure described in **10a** using starting materials 2-chloro-1-(8-methylimidazo[1,2-a]pyridin-3-yl)ethanone **3b** and *N,N*-dimethyl-*N'*-(tritylcarbamothioyl)formimidamide **8**. **10n** was purified by column chromatography (Hexane: Ethyl acetate = 2:8). Pale yellow solid; Yield: 60%; Purity: 99.5%; Melting point: 194–196 °C; Molecular formula: C₁₂H₁₀N₄O₂S; LC-ESI-MS (*m/z*): 259.2 [M+H]⁺; IR (KBr, cm⁻¹): 3493.09, 3373.50, 3064.80, 1664.57; ¹H NMR (400 MHz, DMSO-*d*₆): δ 2.580 (s, 3H); δ 7.128 (t, *J* = 6.8 Hz, 1H); δ 7.4205 (d, *J* = 6.8 Hz, 1H); δ 8.054 (s, 1H), 8.090 (s, D₂O exchangeable, 2H); δ 8.526 (s, 1H) δ 9.2735 (d, *J* = 6.8 Hz, 1H); ¹³C NMR (100 MHz, DMSO-*d*₆): δ 16.40, 114.74, 122.68, 125.68, 126.89, 127.07, 127.45, 140.71, 147.64, 147.87, 173.41, 173.66.

4.2.5.15. (2-aminothiazol-5-yl)(7-methylimidazo[1,2-a]pyridin-3-yl)methanone (10o). Final compound **10o** was synthesized as per the procedure described in **10a** using starting materials 2-chloro-1-(7-methylimidazo[1,2-a]pyridin-3-yl)ethanone **3c** and *N,N*-dimethyl-*N'*-(tritylcarbamothioyl)formimidamide **8**. **10o** was purified by column chromatography (Hexane: Ethyl acetate = 2:8). Colorless solid; Yield: 77%; Purity: 99.9%; Melting point: 196–198 °C; Molecular formula: C₁₂H₁₀N₄O₂S; LC-ESI-MS (*m/z*): 259.2 [M+H]⁺; IR (KBr, cm⁻¹): 3432.51, 3342.87, 3085.44, 1664.75; ¹H NMR (400 MHz, DMSO-*d*₆): δ 2.472 (s, 3H), δ 7.136 (d, *J* = 7.2 Hz, 1H), δ 7.481 (s, 1H), δ 7.614 (s, 1H), δ 8.038 (s, D₂O exchangeable, 2H), 8.575 (s, 1H), δ 9.313 (d, *J* = 6.4 Hz, 1H); ¹³C NMR (100 MHz, DMSO-*d*₆): δ 18.42, 115.01, 122.74, 124.97, 125.78, 127.12, 127.93, 141.02, 148.22, 149.31, 171.23, 178.58.

4.2.5.16. (2-aminothiazol-5-yl)(6-methylimidazo[1,2-a]pyridin-3-yl)methanone (10p). Final compound **10p** was synthesized as per the procedure described in **10a** using starting materials 2-chloro-1-(6-methylimidazo[1,2-a]pyridin-3-yl)ethanone **3d** and *N,N*-dimethyl-*N'*-(tritylcarbamothioyl)formimidamide **8**. **10p** was purified by column chromatography (Hexane: Ethyl acetate = 2:8). Colorless solid; Yield: 67%; Purity: 99.9%; Melting point: 202–204 °C; Molecular formula:

C₁₂H₁₀N₄O₂S; LC-ESI-MS (*m/z*): 259.2 [M+H]⁺; IR (KBr, cm⁻¹): 3383.14, 3302.13, 3089.96, 1627.92; ¹H NMR (400 MHz, DMSO-*d*₆): δ 2.378 (s, 3H); δ 7.468 (d, *J* = 8.8 Hz, 1H); δ 7.7385 (d, *J* = 9.2 Hz, 1H); δ 8.045 (s, 1H), 8.075 (s, D₂O exchangeable, 2H); δ 8.505 (s, 1H) δ 9.262 (s, 1H); ¹³C NMR (100 MHz, DMSO-*d*₆): δ 17.78, 124.53, 125.57, 126.68, 127.06, 127.53, 127.66, 131.84, 146.70, 147.46, 147.56, 173.52.

4.3. Animals

In vivo work was carried out using Sprague-Dawley rats (either sex, 150–200 g) (3 animals per cage). Animals were kept in animal house of B. V. Patel PERD Centre under standard conditions (Relative humidity: 60 ± 5%, Temperature: 25 ± 3 °C, 10% air exhaust conditioning unit, 12 h light/dark cycle). Good Laboratory Practice (GLP) mentioned in CPCSEA guidelines were followed for housing and handling of animals. All the experiments were performed after the approval of Institutional Animal Ethics Committee (Approval No: PERD/IAEC/2016/049 & PERD/IAEC/2016/050).

4.4. Anti-inflammatory activity

4.4.1. Carrageenan induced rat paw edema model for acute inflammation

A series of 16 compounds were tested for their acute anti-inflammatory activity using carrageenan induced rat paw edema model. Animals were randomly grouped in to 19 groups (n = 6). These groups were denoted as normal control (NC), disease control (DC), positive control (PC) and 16 test groups (**10a–10p**). Test group (50 mg/kg body weight) and PC group (Diclofenac: 7.5 mg/kg body weight) animals were orally pre-dosed using a suspension of 0.2% agar. NC and DC group animals were received 0.2% agar only. Rat paw edema was induced by 0.1 mL of 1% carrageenan, prepared in normal saline (subcutaneously). The injection was given after 1 h of oral dosing into the left hind paw (sub plantar region) of each rat. Paw volumes were measured using mercury plethysmometer before and after 3 h of carrageenan injection.^{26–28} The reduction in volume of paw edema was calculated as percentage (%) edema inhibition using following equation.

$$\% \text{ edema inhibition} = (V_t/V_0)_{\text{DC}} - (V_t/V_0)_{\text{treated}} / (V_t/V_0)_{\text{DC}} \times 100$$

V_t = rat paw volume at 3rd hour

V₀ = rat paw volume at 0th hour

The results of % edema inhibition are presented as mean ± SEM (n = 6 animals/group). The statistical analysis was performed by one-way ANOVA followed by Tukey's multiple comparison test (*p < 0.05).

4.4.2. Formalin induced rat paw edema model for chronic inflammation

Chronic anti-inflammatory study was carried out using six groups NC, DC, PC and 3 test groups (n = 6). Animals were pre dosed with test compounds (50 mg/kg body weight), celecoxib (positive control, 40 mg/kg body weight) and vehicle (normal control) prepared in 0.2% agar. After 1 h of oral dosing, 0.1 mL of 2% formalin, prepared in normal saline was injected in the sub plantar region of rat's left hind paw (subcutaneously) for consecutive 5 days. After 5 h, the changes in paw volume were recorded using mercury plethysmometer for each day.^{26–28} % edema reduction was calculated using following equation.

$$\% \text{ edema inhibition} = (V_t/V_0)_{\text{DC}} - (V_t/V_0)_{\text{treated}} / (V_t/V_0)_{\text{DC}} \times 100$$

V_t = rat paw volume at 5th hour

V₀ = rat paw volume at 0th hour

The results of % edema inhibition are presented as mean ± SEM (n = 6 animals/group). The statistical analysis was performed by one-way ANOVA followed by Tukey's multiple comparison test (*p < 0.05).

4.5. $AlCl_3$ induced Alzheimer's disease model

Animals were divided into 4 groups NC, DC, PC and test group (n = 6). Animals were pre-dosed with normal saline (for NC and DC), Meloxicam (5 mg/kg body weight, for PC) and test compound (**10c**, 50 mg/kg body weight) using 0.2% agar suspension for 28 days. DC, PC and test group animals were injected with aluminium chloride (4.2 mg/kg, *i.p.*) for 28 days, after oral dosing. NC group received vehicle only.^{31,32} Various studies were performed during this 28 days as described in following procedures.

4.5.1. Behavioral study

Training was given to each animal prior to the $AlCl_3$ dosing for 5 days. Afterwards, behavioral parameters were observed during 28 days of $AlCl_3$ induced AD model using elevated plus maze, pole climbing apparatus and Y maze.

4.5.1.1. Elevated plus maze test. Spatial working memory of rats can be assessed by elevated plus maze test (EPM). It is a natural tendency of rats to be in the safe closed environment rather than an open heighted environment. In this test, rat's ability to remember closed arm location was determined. EPM was made up of two open arms (29 × 5 cm), two closed arms (29 × 5 × 15 cm) and a central platform (5 × 5 cm). This apparatus is placed at the height of 40 cm from the floor. Training session was given for 5 days. During this session, each rat was placed in an open maze away from the central platform and allowed to explore the maze environment for 5 min. The time required for rat to move from an open arm to close arm was recorded as transfer latency.²¹ Same procedure was employed during retention session at 7th, 14th, 21st and 28th day of $AlCl_3$ model. Transfer latency (in seconds) was recorded for each rat.^{27,28} Data are given as mean transfer latency (sec) ± SEM and statistical analysis was performed by two-way ANOVA test followed by multiple comparisons of Tukey's test. Statistical significance was measured as *p < 0.05 compared to NC and as #p < 0.05 compared to DC.

4.5.1.2. Conditioned avoidance response (CAR) rat model. Cognitive function of rats was determined using Cook's pole climbing apparatus. A wooden sound proof apparatus with 25 × 25 × 25 cm dimensions was used for the study. The chamber has metallic grid floor that conduct electric shock. A wooden pole of diameter 2.5 cm was placed on the center of the apparatus. Initially, an animal was placed and allowed to explore the environment of the apparatus for 45 sec. Conditioned stimulus (buzzer signal) and unconditioned stimulus (electric shock) was given through grid floor for 45 sec. All the animals were trained before the actual experiment.²² Acquisition session was given to each animal for 3 days (1st day 5 trials, 2nd day 3 trials and 3rd day 1 trial). During the training session, animals learned to escape from the electric shock by climbing to wooden pole after buzzer signal. Afterwards, 1 trial of CAR was noted for each animal during 7th, 14th, 21st and 28th day of $AlCl_3$ model.^{27,28} Data are represented as mean ± SEM and statistical analysis was performed by two-way ANOVA test followed by multiple comparisons of Tukey's test. Statistical significance was measured as *p < 0.05 compared to NC and #p < 0.05 compared to DC.

4.5.1.3. Y maze test. Y-maze test was used to assess immediate working memory of rats. It is a natural tendency of rodent's to explore novel environment. This test emphasis on this tendency of rodents and calculated in terms of 'simultaneous alteration performance' (SAP). In this test, Y-maze apparatus was used which was made up of 3 identical wooden arms (40 × 9 × 16 cm) denoted as 'A', 'B', and 'C'. These arms were placed at an angle of 120° with respect to each other. A rat was placed in one of the arm and allowed it to explore the environment of maze for 5 min. Rats generally chose to visit unexplored arm over previously visited arm. Arm entries visited by each rat were recorded and

calculated as SAP. SAP was measured as total number of entries minus two. % alteration was measured as (actual correct alteration ÷ maximum alteration) × 100.²³ Rats were trained for consecutive 5 days and % alteration was calculated at 7th, 14th, 21st and 28th day of $AlCl_3$ model.^{27,28} Data are given as mean % alteration ± SEM and statistical analysis was performed by two-way ANOVA test followed by multiple comparisons of Tukey's test. Statistical significance was measured as *p < 0.05 compared to NC and as #p < 0.05 compared to DC.

4.5.2. Haematological parameters estimation

After 28 days of $AlCl_3$ treatment, blood samples were collected from the retro orbital sinus of rats on 29th day. For haematological studies, rats were anaesthetized by isoflurane and blood samples were collected in 1 mL heparinized micro centrifuge tubes. Haemoglobin and haematocrit level were determined using automated haematology analyser (VetScan HM-5; Abaxis Inc., Union City, CA, USA).²⁹

4.5.3. Serum biochemical assays

Rats were anaesthetized using isoflurane and blood samples were collected in 1 mL non-heparinized micro centrifuge tubes from retro orbital sinus. Serum was collected from the blood samples. Biochemical parameters, % albumin and total protein was determined by automated analyser (Transasia EM 360).²⁹

4.5.4. Anti-oxidant activity

After 28 days of $AlCl_3$ model, on 29th day all the rats were euthanized and intact brain was removed. Brains were washed with saline to remove traces of blood. Estimation of lipid peroxidase and superoxide dismutase assays were performed using brain tissues.

4.5.4.1. Lipid peroxidase (LPO) assay. Brain tissues obtained from each group were taken into 5 mL of Hank's balanced salt solution (HBSS, pH 7.4). These tissues were homogenized at 5000 rpm of 3 cycles (30 sec of each cycle) using Polytron homogenizer (Kinematica, Switzerland). Further, homogenates were centrifuged at 35,000 rpm for 10 min using sorvall, legend X1R centrifuge. After that, supernatant was discarded from each sample and pellet was re-suspended in 0.1 mL of HBSS for further use. LPO activity was determined based on the reaction of malonaldehyde (MDA): thiobarbituric acid (TBA). The previously processed tissue homogenate was taken to initiate the reaction. The assay reaction also contained 2 mL of 8.1% of sodium dodecyl sulfate, 1.5 mL of 20% acetic acid (pH 3.5 was adjusted using 1 M NaOH), and TBA (1.5 mL of 0.8% aqueous solution). The final assay volume was made up to 4 mL by addition of 0.7 mL double distilled water. Then, reaction mixture was heated for 1 h at 95 °C in a water bath. After heating, double distilled water (1 mL) and 15:1 v/v n-butanol: pyridine mixture (5 mL) was added and vortexed for 5 min. After that, reaction mixture was centrifuged at 3000 rpm for 7 min and supernatant (organic) was taken and processed further for MDA calculation. MDA formed in reaction mixture was measured using an Ultra violet/Visible Spectrophotometer (Shimadzu UV-1800) at 532 nm. LPO was calculated using MDA extinction coefficient (1.45 × 10⁻⁵/min/cm).^{8,29}

LPO was calculated using following formula:

$$LPO = [(Sample-Blank) \times 145] \times 10^{-5} / \text{weight of organ (grams)}$$

4.5.4.2. Superoxide dismutase (SOD) assay. SOD activity was measured using brain tissues. Tissues were taken in 2 mL of chilled 50 mM Tris buffer (pH 8.2 was adjusted by 2 mM EDTA). Afterwards, tissues were homogenized using 3 cycles of 30 s. Tissue homogenate was treated with 1 mL of 0.1% Triton X 100 (v/v) at 4 °C for 30 min. Further, reaction mixture was centrifuged at 5600 rpm for 30 min (temperature: 4 °C). Supernatant was taken and divided into two parts. One part of supernatant was stored at 4–8 °C and other part was heated at 95 °C for 1 h.

Pyrogallol was added to each reaction to determine SOD activity. Absorbance was recorded on 0th and 9th min of pyrogallol addition at 420 nm. All the calculations were made in terms of per gram fresh tissue weight.^{30,32} SOD enzyme activity was calculated by following equation:

$$\text{Enzyme activity (Units/mg of fresh tissue weight)} = \Delta B - \Delta E / \Delta P * 120$$

where, ΔB = Boiled sample absorbance per min (9th reading – 0th reading)

ΔE = Cold sample absorbance per min (9th reading– 0th reading)

ΔP = Pyrogallol Control per min (9th reading – 0th reading)

4.5.5. Histopathological studies of brain samples

Intact brains were isolated and stored in 10% neutral buffered formalin solution for 24 h. Brain sections were stained by Congo red and haematoxylin-eosin (HE). The slides were observed under optical microscope (ProgRes C3 OLYMPUS, U-TV1 X, Japan) and images were taken using Progrescapture Pro 2.9.0.1 software.

4.5.6. Gastro-intestinal (GI) safety study of compound 10c

Gastrointestinal (GI) safety study was performed for the compound 10c as many anti-inflammatory compounds are reported to show GI toxicity in higher doses. Abdomen of each euthanized rat was opened and stomach and intestines were taken from that. They were washed with cold phosphate buffer saline (0.01 M, at pH 7.4) and stored in sterile tubes. Stomach and intestine samples were kept for 24 h in 10% neutral buffered formalin. After that, samples were washed with 70% ethanol and observed for the hemorrhagic damage using digital vernier caliper (Absolute AOS Digimatic; Mitutoyo, Japan). Lesion index was calculated for stomach and intestinal samples. Stomach and intestinal damage was observed in the HE stained samples using optical microscope.^{24,25}

Declaration of Competing Interest

The authors declare that they have no known competing financial interests or personal relationships that could have appeared to influence the work reported in this paper.

Acknowledgements

All authors thank B. V. Patel Pharmaceutical Education and Research Development (PERD) Centre for providing research facilities. S.R.S. thanks DST-INSPIRE for providing fellowship to carry out research work. S.R.S. thank NIRMA University for registering as research scholar.

Funding Sources

Authors thank B. V. Patel Pharmaceutical Education and Research Development (PERD) Centre for financial support. SRS thanks DST-INSPIRE, Govt. of India for providing fellowship to carry out research work.

Appendix A. Supplementary material

¹H NMR, ¹³C NMR, D₂O exchange and HRMS spectra of compound 10b, ¹H NMR and ¹³C NMR spectra of compounds 10e, 10h and 10m and HPLC chromatogram of compound 10c are provided in Supplementary Material Supplementary data to this article can be found online at <https://doi.org/10.1016/j.bmc.2021.116091>.

References

- Masters CL, Bateman R, Blennow K, Rowe CC, Sperling RA, Cummings JL. Alzheimer's disease, 15056–15056 *Nat Rev Dis Primers*. 2015;1. <https://doi.org/10.1038/nrdp.2015.56>.
- World Health Organization, 2020. <https://www.who.int/news-room/fact-sheets/detail/dementia>, accessed on 29 January 2020.
- Corbett A, Pickett J, Burns A, et al. Drug repositioning for Alzheimer's disease. *Nat Rev Drug Discovery*. 2012;11(11):833–846. <https://doi.org/10.1038/nrd3869>.
- Ferreira ST, Clarke JR, Bomfim TR, De Felice FG. Inflammation, defective insulin signaling, and neuronal dysfunction in Alzheimer's disease. *Alzheimer's & Dementia*. 2014;10:S76–S83. <https://doi.org/10.1016/j.jalz.2013.12.010>.
- Wyss-Coray T. Inflammation in Alzheimer disease: driving force, bystander or beneficial response? *Nat Med*. 2006;12(9):1005–1015. <https://doi.org/10.1038/nm1484>.
- Stalder A. Neuroinflammatory mechanisms in Alzheimer's Disease: basic and clinical research. *Gerontology*. 2002;48(6):409.
- Gökhan-Kelekçi N, Yabanoğlu S, Küpeli E, et al. A new therapeutic approach in Alzheimer disease: some novel pyrazole derivatives as dual MAO-B inhibitors and antiinflammatory analgesics. *Bioorg Med Chem*. 2007;15(17):5775–5786. <https://doi.org/10.1016/j.bmc.2007.06.004>.
- Parekh KD, Dash RP, Pandya AN, Vasu KK, Nivsarkar M. Implication of novel bis-imidazopyridines for management of Alzheimer's disease and establishment of its role on protein phosphatase 2 A activity in brain. *J Pharm Pharmacol*. 2013;65(12):1785–1795. <https://doi.org/10.1111/jphp.12149>.
- Vanda D, Zajdel P, Soural M. Imidazopyridine-based selective and multifunctional ligands of biological targets associated with psychiatric and neurodegenerative diseases. *Eur J Med Chem*. 2019;181:111569. <https://doi.org/10.1016/j.ejmech.2019.111569>.
- Mader M, de Dios A, Shih C, et al. Imidazolyl benzimidazoles and imidazo [4, 5-b] pyridines as potent p38 α MAP kinase inhibitors with excellent in vivo antiinflammatory properties. *Bioorg Med Chem Lett*. 2008;18(1):179–183. <https://doi.org/10.1016/j.bmcl.2007.10.106>.
- Chen G, Liu Z, Zhang Y, et al. Synthesis and anti-inflammatory evaluation of novel benzimidazole and imidazopyridine derivatives. *ACS Med Chem Lett*. 2013;4(1):69–74. <https://doi.org/10.1021/ml300282t>.
- Franklin PX, Pillai AD, Rathod PD, et al. 2-Amino-5-thiazolyl motif: A novel scaffold for designing anti-inflammatory agents of diverse structures. *Eur J Med Chem*. 2008;43(1):129–134. <https://doi.org/10.1016/j.ejmech.2007.02.008>.
- Giri RS, Thaker HM, Giordano T, et al. Design, synthesis and characterization of novel 2-(2, 4-disubstituted-thiazole-5-yl)-3-aryl-3H-quinazolin-4-one derivatives as inhibitors of NF- κ B and AP-1 mediated transcription activation and as potential anti-inflammatory agents. *Eur J Med Chem*. 2009;44(5):2184–2189. <https://doi.org/10.1016/j.ejmech.2008.10.031>.
- Vasu KK, Digwal CS, Pandya AN, et al. Imidazo [1, 2-a] pyridines linked with thiazoles/thiophene motif through keto spacer as potential cytotoxic agents and NF- κ B inhibitors. *Bioorg Med Chem Lett*. 2017;27(24):5463–5466. <https://doi.org/10.1016/j.bmcl.2017.10.060>.
- Kaila JC, Baraiya AB, Pandya AN, Jalani HB, Sudarsanam V, Vasu KK. A convenient one-pot synthesis of trisubstituted 1, 3, 5-triazines through intermediary amidinothioureas. *Tetrahedron Lett*. 2010;51(11):1486–1489. <https://doi.org/10.1016/j.tetlet.2010.01.034>.
- Kaila JC, Baraiya AB, Pandya AN, Jalani HB, Vasu KK, Sudarsanam V. A convenient synthesis of di-and trisubstituted 2-aminoimidazoles from 1-amidino-3-tritylthioureas. *Tetrahedron Lett*. 2009;50(27):3955–3958. <https://doi.org/10.1016/j.tetlet.2009.04.083>.
- Wallace JL, Bak A, McKnight W, Asfaha S, Sharkey KA, MacNaughton WK. Cyclooxygenase 1 contributes to inflammatory responses in rats and mice: implications for gastrointestinal toxicity. *Gastroenterology*. 1998;115(1):101–109. [https://doi.org/10.1016/s0016-5085\(98\)70370-1](https://doi.org/10.1016/s0016-5085(98)70370-1).
- Patil KR, Mahajan UB, Unger BS, et al. Animal models of inflammation for screening of anti-inflammatory drugs: Implications for the discovery and development of phytopharmaceuticals. *Int J Mol Sci*. 2019;20(18):4367. <https://doi.org/10.3390/ijms20184367>.
- Khan AA, Iadarola M, Yang HYT, Dionne RA. Expression of COX-1 and COX-2 in a clinical model of acute inflammation. *J Pain*. 2007;8(4):349–354. <https://doi.org/10.1016/j.jpain.2006.10.004>.
- Yu L, Jiang R, Su Q, Yu H, Yang J. Hippocampal neuronal metal ion imbalance related oxidative stress in a rat model of chronic aluminum exposure and neuroprotection of meloxicam. *Behav Brain Funct*. 2014;10(1):1–10. <https://doi.org/10.1186/1744-9081-10-6>.
- Liu L, Orozco LJ, Planel E, et al. A transgenic rat that develops Alzheimer's disease-like amyloid pathology, deficits in synaptic plasticity and cognitive impairment. *Neurobiol Dis*. 2008;31(1):46–57. <https://doi.org/10.1016/j.nbd.2008.03.005>.
- Wadenberg MLG, Hicks PB. The conditioned avoidance response test re-evaluated: is it a sensitive test for the detection of potentially atypical antipsychotics? *Neurosci Biobehav Rev*. 1999;23(6):851–862. [https://doi.org/10.1016/S0149-7634\(99\)00037-8](https://doi.org/10.1016/S0149-7634(99)00037-8).
- Suo Z, Cox AA, Bartelli N, et al. GRK5 deficiency leads to early Alzheimer-like pathology and working memory impairment. *Neurobiol Aging*. 2007;28(12):1873–1888. <https://doi.org/10.1016/j.neurobiolaging.2006.08.013>.
- Singh DP, Borse SP, Nivsarkar M. Co-administration of quercetin with pantoprazole sodium prevents NSAID-induced severe gastroenteropathic damage efficiently: Evidence from a preclinical study in rats. *Exp Toxicol Pathol*. 2017;69(1):17–26. <https://doi.org/10.1016/j.etp.2016.10.004>.

- 25 Singh DP, Borse SP, Nivsarkar M. Overcoming the exacerbating effects of ranitidine on NSAID-induced small intestinal toxicity with quercetin: Providing a complete GI solution. *Chem Biol Interact.* 2017;272:53–64. <https://doi.org/10.1016/j.cbi.2017.04.006>.
- 26 Pillai AD, Rathod PD, Franklin PX, et al. Novel drug designing approach for dual inhibitors as anti-inflammatory agents: implication of pyridine template. *Biochem Biophys Res Commun.* 2003;301(1):183–186. [https://doi.org/10.1016/S0006-291X\(02\)02996-0](https://doi.org/10.1016/S0006-291X(02)02996-0).
- 27 Sagar SR, Singh DP, Das RD, et al. Pharmacological investigation of quinoxaline-bisthiazoles as multitarget-directed ligands for the treatment of Alzheimer's disease. *Bioorg Chem.* 2019;89:102992. <https://doi.org/10.1016/j.bioorg.2019.102992>.
- 28 Sagar SR, Singh DP, Panchal NB, et al. Thiazolyl-thiadiazines as Beta Site Amyloid Precursor Protein Cleaving Enzyme-1 (BACE-1) Inhibitors and Anti-inflammatory Agents: Multitarget-Directed Ligands for the Efficient Management of Alzheimer's Disease. *ACS Chem Neurosci.* 2018;9(7):1663–1679. <https://doi.org/10.1021/acschemneuro.8b00063>.
- 29 Singh DP, Borse SP, Nivsarkar M. A novel model for NSAID induced gastroenteropathy in rats. *J Pharmacol Toxicol Methods.* 2016;78:66–75. <https://doi.org/10.1016/j.vascn.2015.11.008>.
- 30 Marklund S, Marklund G. Involvement of the superoxide anion radical in the autoxidation of pyrogallol and a convenient assay for superoxide dismutase. *Eur J Biochem.* 1974;47(3):469–474.
- 31 Rather MA, Thenmozhi AJ, Manivasagam T, Bharathi MD, Essa MM, Guillemin GJ. Neuroprotective role of Asiatic acid in aluminium chloride induced rat model of Alzheimer's disease. *Front Biosci (Schol Ed).* 2018;10:262–275. <https://doi.org/10.2741/s514>.
- 32 Zhao Y, Dang M, Zhang W, et al. Neuroprotective effects of Syringic acid against aluminium chloride induced oxidative stress mediated neuroinflammation in rat model of Alzheimer's disease. *J Funct Foods.* 2020;71:104009. <https://doi.org/10.1016/j.jff.2020.104009>.